United States
Department of
Agriculture

Forest Service

**Forest
Products
Laboratory**

Research
Paper

FPL 368

May 1980

Effect of Cross Grain on Stress Waves in Lumber

Abstract

An evaluation is made of the effect of cross grain on the transit time of longitudinal compression stress waves in Douglas-fir 2 by 8 lumber. Cross grain causes the stress wave to advance with a front or contour skewed in the direction of the grain angle, rather than to advance with a front normal to the long axis of lumber. Thus, the timing of the stress wave in lumber with cross grain is complicated. Based on the static bending modulus of elasticity of the lumber evaluated, an average of transit times for determining a stress wave modulus of elasticity (E) was better than two other timing bases. Another timing basis, however, was best in accounting for stress-wave measurements on 2 by 4's cut with a 4.4° slope of grain bias from the 2 by 8's. These results should aid in the development of lumber stress grading systems using E measurements based on stress waves.

United States Department of Agriculture

Forest Service

Forest Products Laboratory[1]

Research Paper

FPL 368

May 1980

Effect of Cross Grain on Stress Waves in Lumber

By
C. C. GERHARDS, Engineer

Introduction

Electromechanical machines are the primary means for machine stress grading lumber, although some specialty grading is done on a long span basis using longitudinal compression stress waves. As in all technological developments of this type, stress-wave grading systems can be made more efficient as measurement interactions with lumber characteristics are better understood. Such efficiency could be advantageous as stress waves offer several potential advantages over mechanical stress raters, including a more rapid throughput, lower induced fiber stress, and lower cost.

In applying longitudinal stress wave theory to wood *(1, 2),*[2] common practice assumes that the stress-wave front is normal to the direction of travel, as in a long slender rod, and that the elementary stress-wave equation (from 6)

$$E = \rho c^2, \quad (1)$$

where E is modulus of elasticity, p is density, and c is speed of the stress wave, reasonably applies to wood. The theory also assumes homogeneous material. Wood is not homogeneous. As E parallel to the grain is commonly more than ten times the E perpendicular to the grain, stress-wave speed parallel to the grain should be more than three times that perpendicular to the grain. Consequently, for a given period of time, a stress wave should travel much farther along the grain than across the grain, implying that the wave front would not remain normal to the long axis of lumber containing sloping grain.

Therefore, as stress-wave stress grading systems are developed, a fundamental understanding of stress-wave interactions with lumber characteristics such as knots, cross grain, moisture content, and growth rings is desirable. Subjects previously studied include the interaction of stress waves with moisture content *(5)* and annual growth rings *(4)* and a comparison of two types of instruments for measuring stress-wave speed in lumber *(3).* This paper presents an evaluation of the effect of cross grain (fiber or grain angle) on longitudinal compression stress waves in, lumber. The type of warp known as cup is also considered as it was an unintentional variable that tended to interact with the type of stress-wave apparatus used.

Materials and Methods

Specimens

Five Douglas-fir 2 by 8's, flatsawn and 8 feet long, were selected for this study. They each contained spiral grain, a type of cross grain that appears on the wide faces of flatsawn lumber *(8).* The specimens were knot-free with annual growth rings generally parallel to the long axis (less than 2.4° or I in 24 deviation). They were conditioned to equilibrium at 73° F and 50 percent relative humidity prior to testing. Dimensions and weight of each piece were measured after equilibrium. Also, the cupping characteristic of each piece was noted as this was soon observed to be an important variable due to the type of stress-wave apparatus used. Positive cup implied a concave warped bark side surface, negative cup the opposite.

Figure 1 shows specimen marking on the bark side prior to measurements of grain angle, modulus of elasticity (E) in static bending, and stress-wave transit time. The midpoints of the eight l-foot increments are identified by the numbers 1 through 8. These numbers also identify the cross sections (CX) that are made at the foot increment midpoints. Another set of numbers 1 through 8 are used to identify the locations of grid points spaced 15/16 inch apart on the cross sections corresponding to CX3, CX4, CX5, and CX6, making 32 grid points in all.

Grain Angle

Grain angle was measured relative to the long axis of the lumber at the midpoints of the foot increments on both bark side and pith side. The

[1] Maintained in Madison, Wis., in cooperation with the University of Wisconsin.

[2] Italicized numbers in parentheses refer to literature cited at the end of this report.

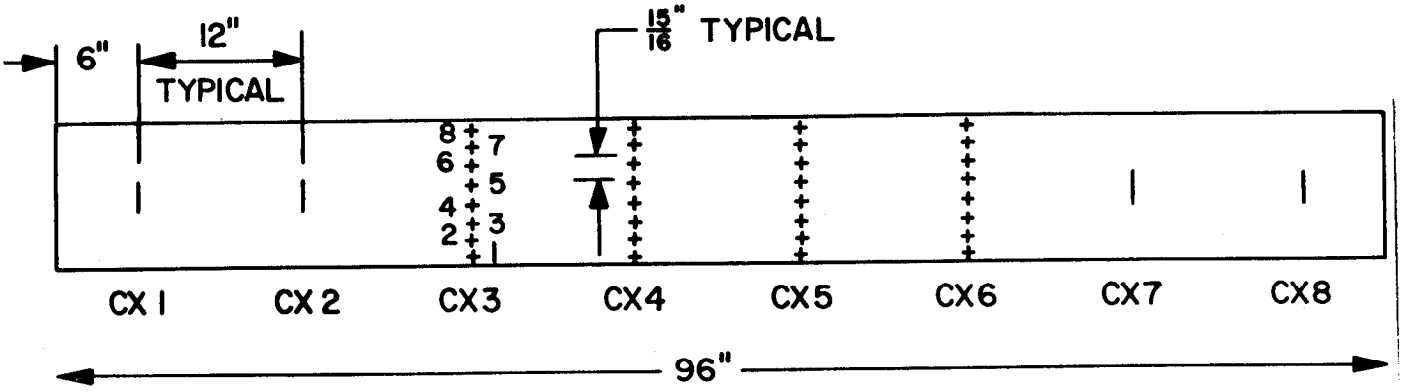

Figure 1.–Markings on the bark side of each specimen-The numbers 1 through 8 identify the midpoints of the 1-foot increments, which also mark the location of cross sections. Another set of numbers 1 through 8 identifies the locations of grid points set 15/16 inch apart on the cross sections. M 148 391

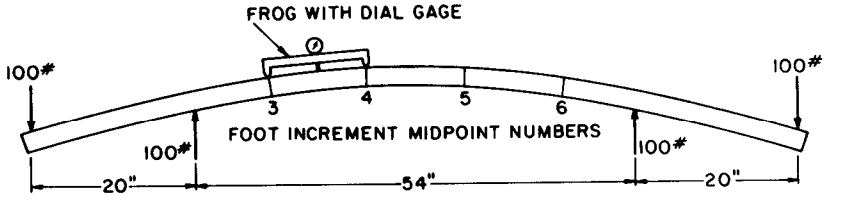

Figure 2.–Schematic of a beam with uniform bending moment over central 54-inch length. Frog with dial gage shown at CX3 to CX4 measures the deflection of the centerpoint relative to CX3 and CX4. M 148 203

grain direction was determined by visual indicators – resin canals, small surface checks, or chipped grain from mill planing.

Static Modulus of Elasticity

A flatwise static bending test was made to determine the static E characteristics of each specimen for later comparison with stress-wave E's In the static test the central 54 inches of specimen length were subjected to a 2,000-inch-pound uniform bending moment as shown in figure 2. The resultant centerpoint deflections for l-foot spans were measured on the upper surface relative to increment midpoints 3 and 4, 4 and 5, and 5 and 6. These deflections were used to calculate three static bending E's per specimen from

$$E = 36{,}000/I\delta \qquad (2)$$

where I is moment of inertia in inches^4 and δ the deflection in inches.

Stress-wave Measurement

Stress-wave transit time to each of the 32 grid points shown in figure 1 was measured with the instrument shown in figure 3 *(5).* With this instrument a compressional stress wave is induced in the end of a specimen by a solenoid-activated hammer striking a steel horn clamped to the hammer end of the specimen. Two accelerometers are fastened to the specimen to sense passage of the induced stress wave. The accelerometer nearer the hammer end starts a microsecond counter; the second accelerometer stops it, thus providing the time for the impact stress wave to go from the first to the second accelerometer. In this study the start or reference accelerometer was clamped on the bark side within 1/4 inch of midwidth (accelerometer clamp did not allow reaching to actual midwidth) 6 inches from the hammer end. The second accelerometer was fastened to each of the barkside grid points in random sequence. Thus, the time for an induced stress wave to reach each grid point was measured relative to a common start accelerometer position. Similarly, the position that gave the shortest transit time of the stress wave, that is, the "fastest point" on each cross section containing grid points, was determined by trial and error searching with the stop accelerometer.

Seven sets of stress-wave times were measured to the 32 grid points on each 2 by 8 (fig. 4). Each set constituted one run. Runs 1 and 3 were made with the end nearer foot increment 1 (number 1 end) toward the hammer, and runs 2 and 4 were made with the end nearer foot increment 8 (number 8 end) toward the hammer. Runs 5, 6, and 7 were oriented in the same direction as runs 1 and 3; but before each of these latter three runs was made, a 6-inch length was sawn off the number 1 end. Thus, by run 7 each specimen had been shortened by 1-1/2 feet as shown schematically in figure 4.

Following run 7, two specimens were cut from each 2 by 8. One was a 6-inch section for determining moisture content (ovendry method) and annual growth rate. The other was a 4-foot long 2 by 4 cut from the number 8 end of each 2 by 8 and oriented to obtain a 4.4° increase in slope of grain (fig. 4). In specimen DF-XG-5, however, the slope was inadvertently decreased by 4.4°. Four grid points spaced 1 inch apart were marked on the bark side of the 2 by 4's at each cross section corresponding to CX5 and CX6 on the 2 by 8's, with the slight adjustment needed to 'make them 1 foot apart. Stress-wave times were measured to each of the 8 grid points on the 2 by 4's with the start accelerometer 6 inches from the end nearer foot increment 8.

Results

Physical *Properties*

The angle of spiral grain varied along the length and from wide face to wide face of each specimen as well as between specimens (table 1). Four of the specimens had slopes

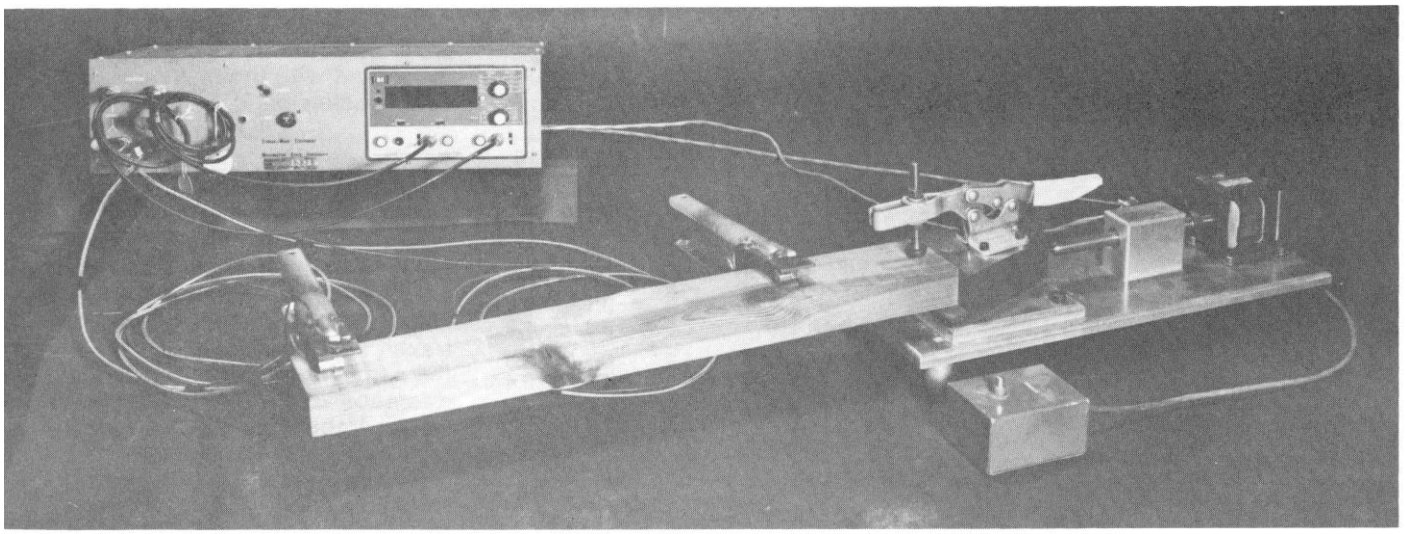

Figure 3.–Stress-wave equipment used to measure transit times in 8-foot 2 by 8's showing the microsecond timer, solenoid impact hammer, steel horn and clamp, and the two accelerometers clamped to a demonstration 2 by 4. M 141 881

caused by left-handed (as in a 'left-handed screw) spiral grain relative to the bark side; the other (DF-XG-2) had right-handed spiral grain. The maximum grain angle measured on the wide faces of each specimen ranged from 6.7° to 9.5° (1 in 8.5 to 1 in 6.0 equivalent slope), while the minimum ranged from 1.9° to 3.5° (1 in 30 to 1 in 16 equivalent slope). Within the seventh 1-foot increment of DF-XG-5, however, there was a steep local deviation to the annual rings, as would occur at a local crook or bulge in a tree.

Several of the other physical properties also varied (table 2). There was considerable variation between the specimens in specific gravity and growth rate and to some extent in static-bending E. Within-specimen variation in static-bending E was small. Moisture content was approximately 11 percent for all specimens. Three of the specimens had positive cup and two negative cup.

Impact Stress-Wave Contours

Cup

Before evaluating the results of stress-wave measurements, it is necessary to consider the difficulty of inducing a uniform contoured longitudinal stress wave into a wide lumber specimen. The interaction between the steel horn clamp of the stress-wave apparatus and specimen cup resulted in a nonuniform induced stress wave. Because a specimen is clamped against a lip (6-in. maximum width) extending from the steel horn, and the end of the specimen is not held tight against the horn, most of the energy of the stress wave must be induced through the lip of the horn. If a specimen is not cupped and not very wide, the induced stress wave should be nearly uniform across the width of the piece at the start. For a wide, cupped specimen, however, the stress wave will be induced at the point of contact between the horn lip and specimen surface. With bark side

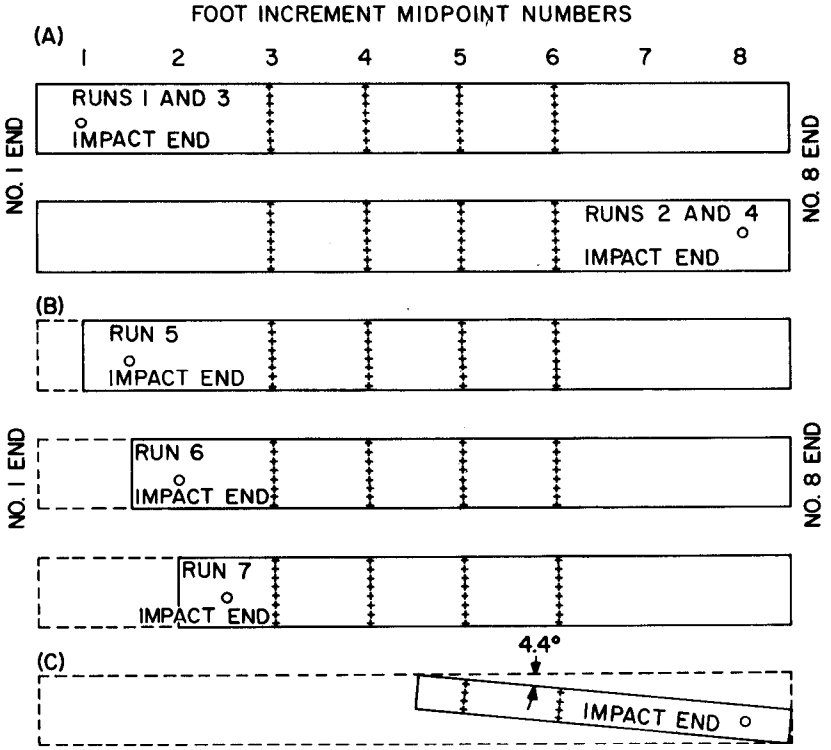

Figure 4.–Diagram showing impact end for runs and the grid points (+) to which transit times were measured. Circled dot indicates B-inch position of first accelerometer from impact end. (A) 2 x 8's 8-foot length, 32 grid points; (B) 2 x 8's, consecutive 6-inch lengths removed, 32 grid points; (C) 2 x 4 cut from 2 x 8 with a 4.4° bias, 8 grid points. M 148 207

Table 1.–Grain angle characteristics on the wide faces of the five Douglas-fir 8-foot long 2 by 8's containing spiral grain[1]

Specimen number	Flatsawn surface	Grain angle in degrees at specimen foot increment numbers							
		1	2	3	4	5	6	7	8
DF-XG-1	Bark side	3.8	4.1	5.6	3.2	3.1	8.7	7.9	8.7
	Pith side	3.6	4.6	4.0	5.2	6.3	6.7	6.3	8.7
[2]DF-XG-2	Bark side	—	6.0	6.9	4.1	3.8	4.6	5.7	5.4
	Pith side	—	4.4	4.6	3.5	3.9	5.0	3.6	3.8
DF-XG-3	Bark side	7.1	7.1	8.7	6.3	5.9	5.2	8.1	9.5
	Pith side	6.0	8.7	7.6	5.4	7.1	6.9	3.8	1.9
DF-XG-4	Bark side	6.2	5.0	2.9	4.4	4.8	5.7	5.1	4.8
	Pith side	6.7	3.5	3.2	4.6	5.2	5.2	4.6	5.4
DF-XG-5	Bark side	—	4.2	5.4	4.4	5.7	9.1	4.4	6.3
	Pith side	—	4.8	5.2	3.0	5.4	6.9	4.1	8.1

[1] A possible three-dimensional effect suggested by the differences in grain angle on bark side and pith side was not evaluated in this study.

[2] Specimen 2 had right-handed spiral grain relative to the bark side, all others had left-handed.

up in the clamped position a positive-cupped specimen will contact the horn lip only at the center, resulting in a stress wave that leads along the center and lags toward the edges. With bark side up in the clamped position a negative-cupped specimen will contact the horn lip toward the edges (lumber wider than the lip) resulting in a stress wave leading toward the edges and lagging toward the center.

Contours at CX3 relative to specimen shortening.

As both positive and negative cupping were encountered (table 2), stress-wave transit time contours leading or lagging along the centerline were both observed as suggested by the examples shown in figure 5. The stress-wave time contours of figure 5 are based on data gathered in runs 1, 5, 6, and 7 at CX3 of specimens DF-XG-4 and DF-XG-5 and were estimated from

$$D_i = d(\bar{t}/t_i) \quad (3)$$

where t_i is measured transit time to a grid point on CX3, $\bar{t}$ is the average of the t_i's for CX3 which is at distance d from the reference accelerometer, and D_i is the calculated distance from the reference (start) accelerometer for a transit time of $\bar{t}$. Run 7, with CX3 located 6 inches from the reference accelerometer (12-in. from the hammer end), best demonstrates the effect of positive cupping in DF-XG-4 and negative cupping in DF-XG-5 on the induced stress wave. Figure 5 shows that the stress wave led near midwidth in DF-XG-4 but lagged near midwidth in DF-XG-5 in run 7. These leading and lagging characteristics diminished the farther CX3 was from the hammer end, apparently due to the influence of cross grain. In run 1, with CX3 at 30 inches from the end, the stress-wave contours in figure 5 are shown leading along grid line 8, consistent with the slope of grain in both specimens.

Contours at CX3, CX4, CX5, and CX6 for the intact specimen

Contours of figure 6, based on data in run 1 and determined similarly to those of figure 5, show that the effect of cross grain became more pronounced with distance of stress-wave transit beyond CX3. At 66 inches from the hammer end (60 in. from the reference accelerometer) the stress-wave contours were generally sloped consistent with the direction of the cross grain-a positive slope in DF-XG-2 consistent with right-handed spiral grain and a negative slope in the other four specimens consistent with left-handed spiral grain. The characteristic trend of the stress-wave at 66 inches from the hammer end results from a wave speed greater when parallel than when perpendicular to grain.

Due to the interaction of specimen cupping and hammer grip, it is difficult to relate the magnitudes of the slopes of stress-wave contours and cross grain. Specimen DF-XG3 had the steepest general slope of grain up through CX5 (table 1), but the slopes of the stress-wave contours in figure 6 were very similar to those for DF-XG-5. Except at CX1, DF-XG-1 and DF-XG-4 had similar slopes of grain up through CX5, yet the stress-wave contours were much more reflective of cross grain in DF-XG-4, perhaps because the slope of grain was so much greater at CX1.

Table 2.–Physical properties of the five Douglas-fir 8-foot long 2 by 8's containing spiral grain

Specimen number	Moisture content	Specific gravity[1]	Growth Rate, rings per inch	Cup[2]	Static bending E, 10^6 psi[3]			
					Between cross sections			Average
					3 and 4	4 and 5	5 and 6	
	Pct							
DF-XG-1	11	0.52	9	Positive	2.4	2.3	2.2	2.3
DF-XG-2	11	.42	40	Positive	1.6	1.6	1.6	1.6
DF-XG-3	11	.61	16	Negative	1.6	1.8	1.9	1.8
DF-XG-4	10	.39	22	Positive	1.7	1.6	1.8	1.7
DF-XG-5	10	.39	17	Negative	1.6	1.6	1.6	1.6

[1] Test volume, ovendry weight basis.
[2] Positive implies concave bark side surface, negative implies convex.
[3] Uniform bending moment basis.

Pitch pockets

Even small pitch pockets may have an apparent effect on the stress-wave contour, particularly if the stress-wave sensing element falls on wood overgrowing the pocket. DF-XG-2 contained two shallow growths over small pitch pockets-one at CX4, the other at CX5–resulting in longer transit-time readings, and consequent lags in stress-wave contours near midwidth at the two CX's (figure 6).

Different impact end

Based on data obtained in run 2 with the lumber end opposite to that for run 1, that is, with the number 8 end toward the hammer, the stress-wave contours shown in figure 7 reflect somewhat different slope-of-grain characteristics than those in figure 6. The slope of grain was steeper toward the number 8 end than toward the number 1 end in DF-XG-1 and DF-XG-5, but the stress-wave contours only reflect that trend in DF-XG-1. In DF-XG-5 the local steep slope of annual rings at CX 7 had a much greater effect than the spiral grain, producing a very noticeable lag in the stress-wave contour along the lower 15/16-inch grid numbers at CX6 (30 in. from the hammer end). The other three specimens tended to have shallower spiral grain on the number 8 end; their stress-wave contours show the effect of lesser slope at 30 inches from the hammer end in figure 7, as compared to figure 6, consistent with the angle of cross grain.

Matched Run Comparisons

Run 3 yielded results very like run 1, and run 4 very like run 2; however, some differences did exist between matched runs. These differences are reflected in the data of table 3, which are the standard deviations of grid point differences in transit time between matched runs expressed as a percent of the average of measured times to a cross section. The coefficients in table 3 average out to 1.0 percent, but the general increasing trend of coefficients with CX number for matched runs 2 and 4 implies that the relative error of measurement decreased with increasing transit distance. However, no such trend is apparent for matched runs 1 and 3. The maximum microsecond (μs) difference in time measurements to any one grid point between matched runs was 13 μs (less than 6 percent error),

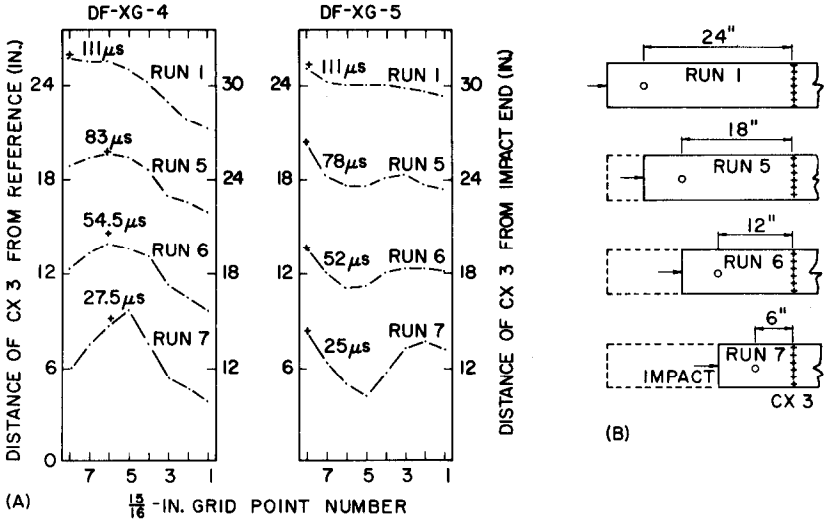

Figure 5.–(A) Calculated stress-wave time contours centered about cross section 3 on the bark side of two 2 by 8's as a function of distance from impact end. DF- XG- 4 had positive cup, DF- XG- 5 had negative cup. (B) Distances from reference point 0 as consecutive 6-inch lengths were removed. M 148 205

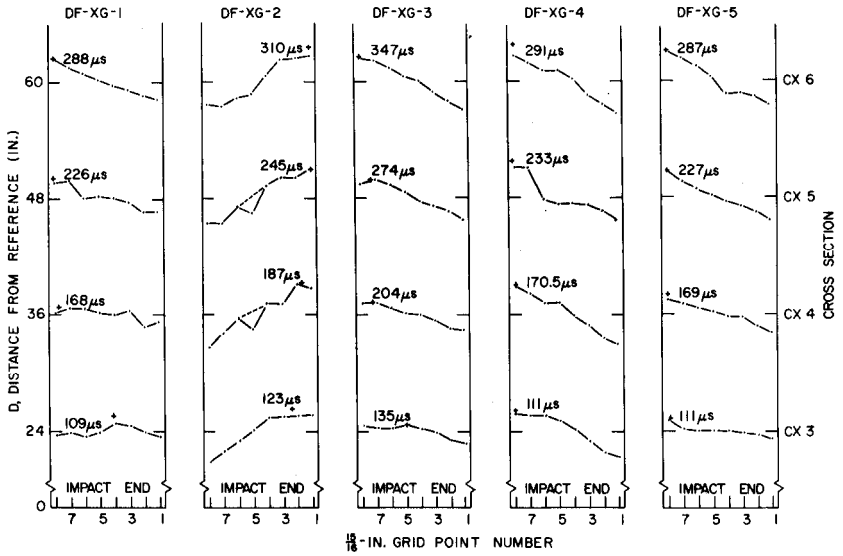

Figure 6.–Calculated stress-wave contours centered about cross sections 3, 4, 5, and 6 on the bark side of five 2 by 8's. M 148 205

which occurred in matched runs 1 and 3 of DF-XG-4.

Fastest Point of Stress Wave

Some small inconsistencies in transit-time data are also apparent in that the fastest point of the stress wave determined by trial and error searching with the accelerometer differs somewhat from the fastest point on the contour calculated from grid-point data. Examples of these inconsistencies are most pronounced in some of the contours for DF-XG4 in figures 5 and 6, for DF-XG-1 and DF-XG-2 in figure 6, and for DF-XG-5 in figure 7 where the trial and error fastest points (+) do not coincide with the contour fastest points. Another item to be noted is that the position of the fastest point of the contours tends toward the edge of a specimen consistent with the direction of grain, except for runs 2 and 4 on DF-XG-5 where it tended to stay near midwidth. The exception is apparently due to the steep local growth ring deviation toward the number 8 end of DF-XG-5.

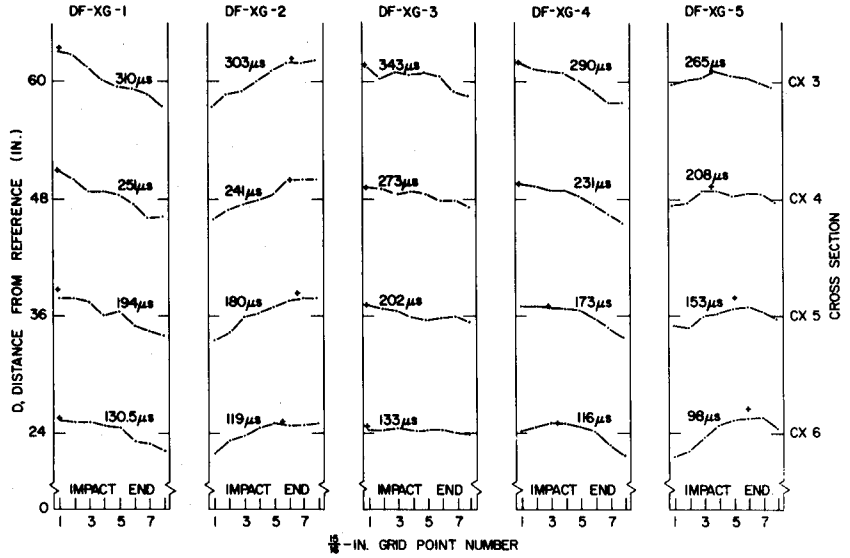

Figure 7.–Calculated stress-wave contours centered about cross sections 3, 4, 5, and 6 as in figure 6 but with opposite end to the impact end. M 148 392

Stress- Wave Timing Bases

Because of the nonuniformity observed in the stress-wave contours, three different bases of timing the stress wave are evaluated: (1) fastest point at a CX; (2) average based on the average of times to the eight grid points of a CX; and (3) centerline based on the average of times to the two grid points near midwidth of a CX.

Stress-wave times for the 3 feet of transit distance between CX3 and CX6 presented in table 4 demonstrate that the shortest transit times occurred for the fastest point basis in all runs for all specimens except for runs 2, 4, and 7 on DF-XG-5. The longest times occurred for the centerline basis except for most of the runs on DF-XG-5 and runs 2, 4, and 7 on DF-XG-3. The different behavior of DF-XG-5 apparently was due to the negative cup on the number 1 end, which caused an early lag in the stress-wave contour near midwidth for run 7, and to the local growth ring slope toward the number 8 end, which apparently had a pronounced effect on the fastest point of the stress wave in runs 2 and 4. The data in table 4 also show that matched runs generally yielded the same times for the 3-foot transit distance with a maximum difference of 5 μs between runs 1 and 3 of DF-XG-2 for the centerline basis. A third point of interest in table 4 is that the times for the 3-foot transit distance depended to some extent on which end of the lumber was impacted. This third point is apparent by comparing runs 1 and 3 with runs 2 and 4 where the absolute differences due to impact end vary from 1 to 9 μs. The general tendency in the end effect is toward higher absolute differences for the centerline timing basis and lower absolute differences for the fastest point basis. Finally, as evidenced by comparing the data for runs 1, 3, 5, 6, and 7, there is no consistent trend in the times for the 3-foot transit distance due to shortening the specimens.

Modulus of Elasticity (E)

As static bending E did not vary greatly over the 3-foot length between CX3 and CX6 (table 2), the average static E given in table 2 for each specimen was used as the basis for comparing E's derived from specimen density and from the stress-wave data of table 4, which covers the same 3-foot length as for static E. Stress-wave E's were calculated from equation (1) where c was obtained by dividing the 3-foot distance by the stress-wave transit time.

The stress-wave E's, derived for the various runs and for the three different timing bases, are summarized in figure 8 as a percent of static bending E. Except for DF-XG-5, stress-wave E's tend to be greatest for the fastest point timing basis and least for the centerline timing basis. Again, except for DF-XG-5, the stress-wave E's based on average time tended to be closer to the static bending E's than either of the other two bases. In fact, the average relative stress-wave E for all seven runs of the first four specimens averaged 99 percent for the average basis compared to 106 percent for the fastest point basis and 96 percent for the centerline basis. For DF-XG-5 stress-wave E was higher than static E in all runs regardless of the timing basis, extending to 21 percent higher for the centerline basis in run 7.

Figure 8 also demonstrates that stress-wave E's were generally close for matched runs, differing by a maximum of 6 percent between runs 1 and 3 for the centerline basis in both DF-XG-1 and DF-XG-5. The end effect on stress-wave E (runs 1 and 3 compared to runs 2 and 4) was not strongly evident for most specimens, but it amounted to about an 11 percent difference for DF-XG-5 by the centerline basis.

Table 3.–Coefficients of variation in measured transit time between matched runs

Specimen number	Cross section	Coefficient of variation in percent	
		Between Runs 1 and 3	Between Runs 2 and 4
DF-XG-1	3	1.3	.7
	4	1.2	1.0
	5	.9	1.0
	6	1.4	1.5
DF-XG-2	3	1.1	.3
	4	2.2	.9
	5	1.4	1.3
	6	1.7	1.6
DF-XG-3	3	.7	.7
	4	.7	.6
	5	.7	.7
	6	1.0	1.0
DF-XG-4	3	.7	.7
	4	1.0	.7
	5	2.0	1.3
	6	.7	1.7
DF-XG-5	3	.5	.6
	4	1.2	.9
	5	.5	1.0
	6	.5	1.8

[1] Based on the standard deviation of differences at eight grid points for each cross section divided by the overall average time for the cross section.

2 by 4 Results

The 2 by 4's were cut to achieve a 4.4° increase in grain angle from that in the 2 by 8's (except for the inadvertent decrease in angle in DF-XG-5). The stress-wave contours for the 2 by 4's at CX6 and CX5 exhibited a more pronounced effect due to grain slope

than did the 2 by 8's. The effect was observed as a strong leading tendency along the edge in the direction of the sloping grain and a lagging tendency along the opposite edge. Due to the increase in grain angle, stress-wave times for the 1-foot transit distance in the 2 by 4's were somewhat higher than those for the 2 by 8's; however, these times did not favor any one particular timing basis as they did for the 3-foot transit distance in the 2 by 8's.

A theoretical effect of a change in grain angle on stress-wave transit time can be calculated based on equation (2) and the equation from March *(7)*

$$\frac{1}{E_\Theta} = \frac{\cos^4\Theta}{E_0} + \frac{\sin^4\Theta}{E_{90}} + \left(\frac{1}{G} - \frac{2\nu}{E_0}\right)\sin^2\Theta\cos^2\Theta \qquad (4)$$

where ? ?is the grain angle, G is shear modulus, ν is Poisson's ratio, and subscripts 0 and 90 refer to parallel and perpendicular grain directions, respectively. E? can be solved if the constants of equation (5) are known, or E? ? can be solved with respect to E_0 if Poisson's ratio and the ratios of E_0 to E_{90} and E_0 to G are known. The latter approach, that is E? /E_0, was taken using $E_{90} = 0.050E_0$, G = $0.078E_0$, ν = 0.449 *(8).* Actually, ν and E_{90} do not have much effect on E? in the range of grain angles encountered in the present lumber sample. Using the above ratios it is possible to calculate an effect on E of changing grain slope from? ? 1 to? ? 2. Then, because E is inversely proportional to the square of transit time, (equation 1), it follows that

$$T_{\Theta 2}/T_{\Theta 1} = \sqrt{E_{\Theta 1}/E_{\Theta 2}} \qquad (5)$$

where T is stress-wave transit time over a specified distance. The actual ratios based on timing of the stress wave between CX6 and CX5 by the fastest point basis agree very favorably with the theoretical ratios based on equations (4) and (5) (table 5). Actual ratios based on average or centerline timing compare less favorably with the theoretical ratios than do the ratios for the fastest point timing basis. The time ratios by the average timing basis would agree more favorably with the theoretical time ratios if the G/E ratio was closer to 0.11 than 0.078. An even larger G/E ratio would be needed to make the centerline timing basis ratios more agreeable with theory.

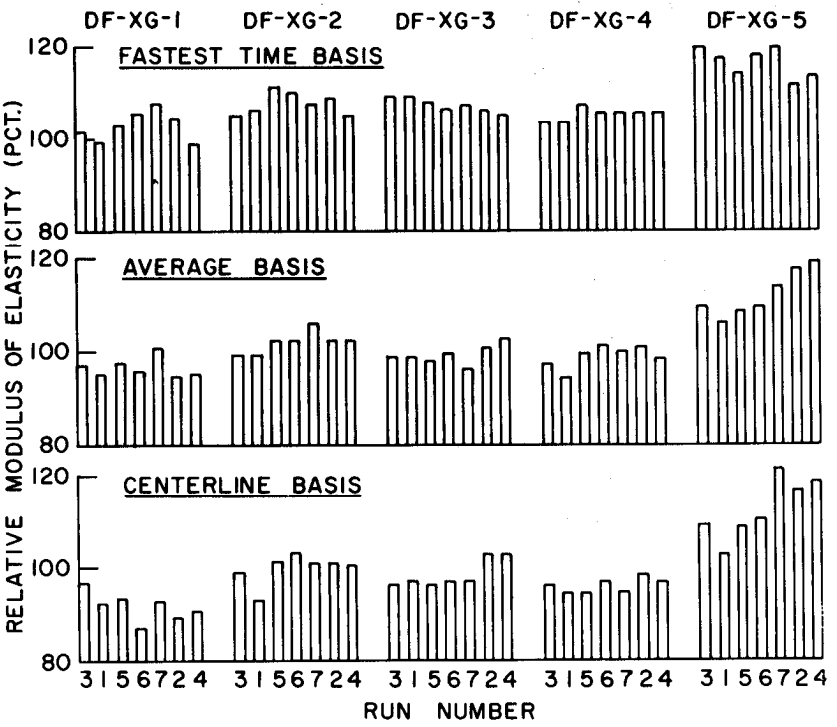

Figure 8.–Stress-wave modulus of elasticity as a percent of static bending modulus of elasticity for the 3-foot length between CX3 and CX6. M 148 393

Table 4.–Stress wave times for a 3- foot transit distance

Specimen number	Timing basis[1]	Transit time in μs between CX 3 and CX 6 for run numbers						
		3	1	5	6	7	2	4
DF-XG-1	Fastest point	173	175	172	170	168	171	176
	Average	177	179	176	178	174	180	179
	Centerline	178	182	180	187	181	184	184
DF-XG-2	Fastest point	182	181	177	178	180	179	182
	Average	187	187	184	184	181	184	184
	Centerline	188	193	186	184	186	186	186
DF-XG-3	Fastest point	202	202	203	205	204	205	206
	Average	212	212	213	212	215	210	208
	Centerline	215	214	214	214	214	208	208
DF-XG-4	Fastest point	172	172	169	170	170	170	170
	Average	177	180	175	174	174	174	176
	Centerline	178	180	180	177	182	176	178
DF-XG-5	Fastest point	166	168	170	167	166	172	171
	Average	173	176	174	173	170	167	166
	Centerline	174	178	174	172	164	168	166

[1] Fastest point implies timing of earliest arrival of stress wave at CX 3 and CX 6. Average is based on timing of stress wave to eight grid points at CX 3 and also at CX 6. Centerline is based on average of stress-wave timing to the two centermost grid points at CX 3 and also at CX 6.

Conclusions

Because stress waves travel faster along the grain than across, longitudinal stress waves in wood tend to lead in the direction of the grain slope. The timing of a stress wave transmitted a certain distance in lumber containing cross grain is somewhat complicated by that trend in that different methods of timing may yield somewhat different results; no differences would be expected if the stress-wave contour remained normal to the direction of transit. Of the three timing bases evaluated, the average basis yielded a stress-wave

modulus of elasticity (E) closest to the static E of the 2 by 8 lumber, while the fastest point basis yielded a stress-wave E more than the static E, and the centerline basis yielded a stress-wave E less than the-static E. On the other hand, results of the fastest point timing basis most closely agreed with the theoretical effect of a 4.4° change in slope of grain. Finally, depending on the apparatus and the presence of positive or negative cup in the specimen, the stress-wave contour induced in the end of lumber may not be normal. particularly in wide specimens, but may lead along either the centerline or near the edges, affecting the shape of stress-wave contours some distance away from the end.

Table L.-Transit time ratios (2 by 4 μs/2 by 8 μs) due to a 4.4° change in grain angle[1]

Specimen number	Theoretical[2]	[3]Actual, based on timing		
		By Fastest point	By Average	By Centerline
DF-XG-1	1.10	1.12	1.06	1.05
DF-XG-2	1.08	1.11	1.06	1.00
DF-XG-3	1.10	1.12	1.06	1.01
DF-XG-4	1.09	1.07	1.08	1.06
DF-XG5	.94	.94	.98	.96

[1] Based on stress wave transit from CX6 to CX5 in the 2 by 8's and in the 2 by 4's cut to effect a 4.4° change in grain angle.
[2] Based on equations (4) and (5) and the average of grain angles at CX5 and CX6.
[3] Based on average of results from runs 2 and 4 at CX 5 and CX 6 on 2 by 8's and the run on 2 by 4's at CX 5 and CX 6.

Literature Cited

1. Bertholf, L. D.
1965. Use of elementary stress wave theory for prediction of dynamic strain in wood. College of Engineering, Wash. State Univ. Bull. No. 291.

2. Galligan, W. L., and R. W. Courteau.
1965. Measurement of the elasticity of lumber with longitudinal stress waves and the piezoelectric effect of wood. Proceedings, 2nd Symposium on the Nondestructive Testing of Wood. Wash. State Univ. p. 223-244.

3. Gerhards, C. C.
1978. Comparison of two nondestructive instruments for measuring pulse transit time in wood. Wood Sci. 11(1):13-16. July.

4. Gerhards, C. C.
1978. Effect of earlywood and latewood on stress wave measurements parallel to the grain. Wood Sci. 11(2):69-72, Oct.

5. Gerhards, C. C.
1975. Stress- wave speed and MOE of sweetgum ranging from 150 to 15 percent MC. For. Prod. J. 25(4):51-57. April.

6. Kolsky, H.
1963. Stress waves in solids. Dover Publications. 213 p.

7. March, H. W.
1944. Stress- strain relations in wood and plywood considered as orthotropic materials. For. Prod. Lab. Rep. No. 1503.

8. U.S. Forest Products Laboratory.
1974. Wood handbook: wood as an engineering material. USDA Agriculture Handbook No. 72, rev.

☆ U.S. GOVERNMENT PRINTING OFFICE: 1960-651-111/4